A

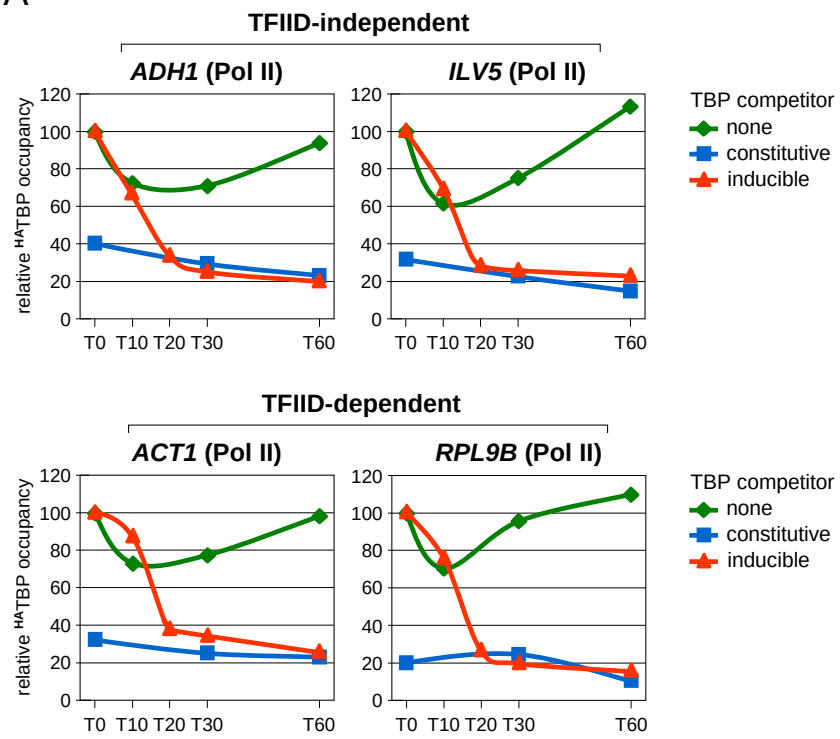
TFIID-independent
ADH1 (Pol II)
ILV5 (Pol II)
relative HATBP occupancy
0
20
40
60
80
100
120
T0 T10 T20 T30 T60
TBP competitor
none
constitutive
inducible
TFIID-dependent
ACT1 (Pol II)
RPL9B (Pol II)

B

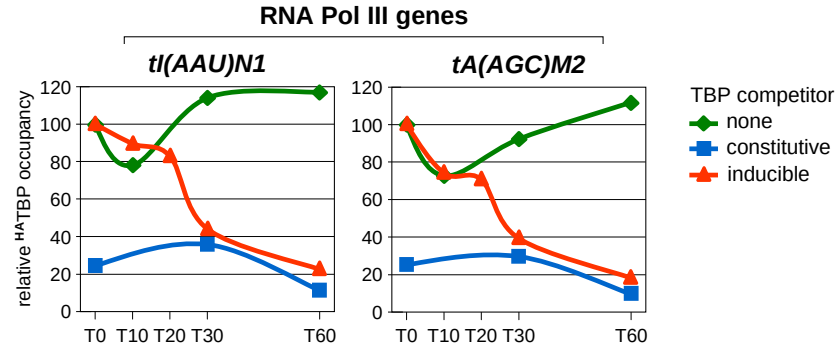
RNA Pol III genes
tI(AAU)N1
tA(AGC)M2
relative HATBP occupancy
0
20
40
60
80
100
120
T0 T10 T20 T30 T60
TBP competitor
none
constitutive
inducible

C

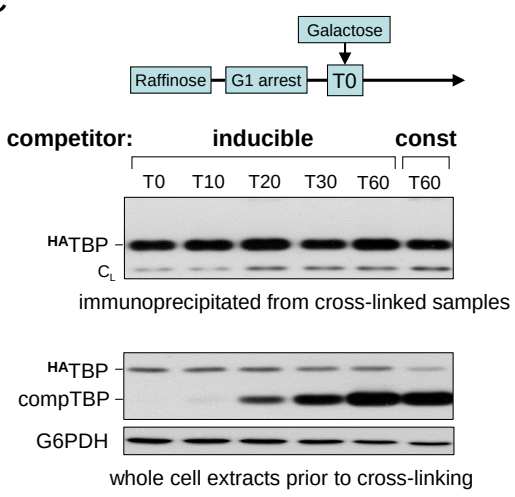
Galactose
Raffinose
G1 arrest
T0
competitor:
inducible
const
T0 T10 T20 T30 T60 T60
HATBP
CL
immunoprecipitated from cross-linked samples
HATBP
compTBP
G6PDH
whole cell extracts prior to cross-linking

Figure S1. TBP turnover at RNA Pol II and RNA Pol III promoters as measured by a ChIP-based competition assay.

(A) The levels of ^{HA}TBP occupancy at the indicated TFIID-independent and TFIID-dependent RNA Pol II promoters and time points (in minutes) were determined in G1-arrested cells by quantitative ChIP analysis as described in Figure 1.

(B) Same as in *(A)* at RNA Pol III promoters.

(C) The same amount of ^{HA}TBP is immunoprecipitated from the cross-linked chromatin samples at all time points after galactose induction of the TBP competitor. Aliquots of the immunoprecipitated chromatin samples used for the ChIP analyses presented in Figures 1D and 1E were loaded before cross-link reversal onto an SDS/polyacrylamide gel and analyzed by western blotting. ^{HA}TBP was detected using anti-HA antibodies. Shown below for comparison is the western blot analysis of ^{HA}TBP and TBP presented in Figure 1C performed with whole cell extracts prepared prior to formaldehyde cross-linking.

A

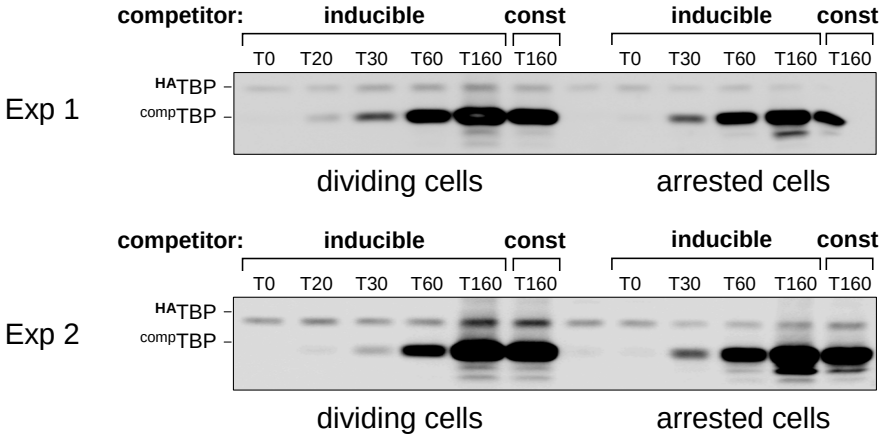
competitor:
inducible
const
inducible
const
T0 T20 T30 T60 T160 T160 T0 T30 T60 T160 T160
HATBP
compTBP
Exp 1
dividing cells
arrested cells
competitor:
inducible
const
inducible
const
T0 T20 T30 T60 T160 T160 T0 T30 T60 T160 T160
HATBP
compTBP
Exp 2
dividing cells
arrested cells

B

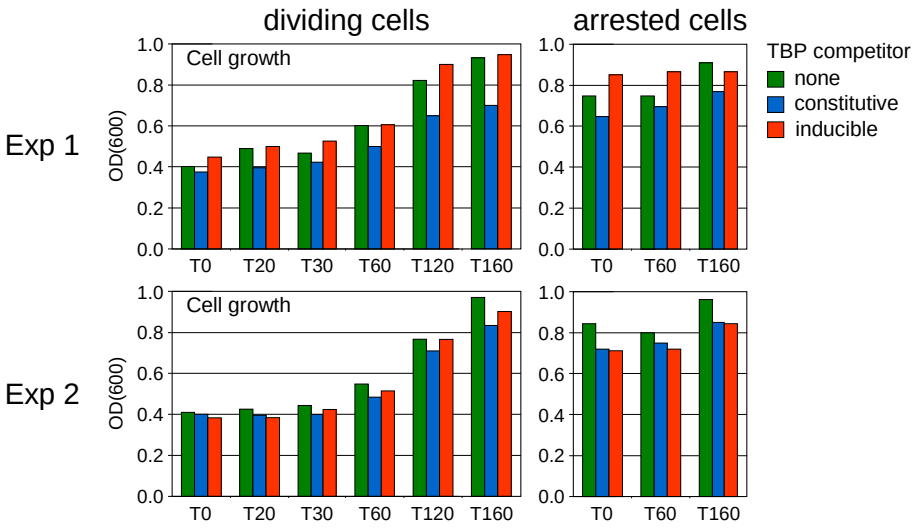
dividing cells
arrested cells
Exp 1
Cell growth
OD(600)
1.0
0.8
0.6
0.4
0.2
0.0
T0 T20 T30 T60 T120 T160
T0 T60 T160
TBP competitor
none
constitutive
inducible
Exp 2
Cell growth
OD(600)
T0 T20 T30 T60 T120 T160
T0 T60 T160

C

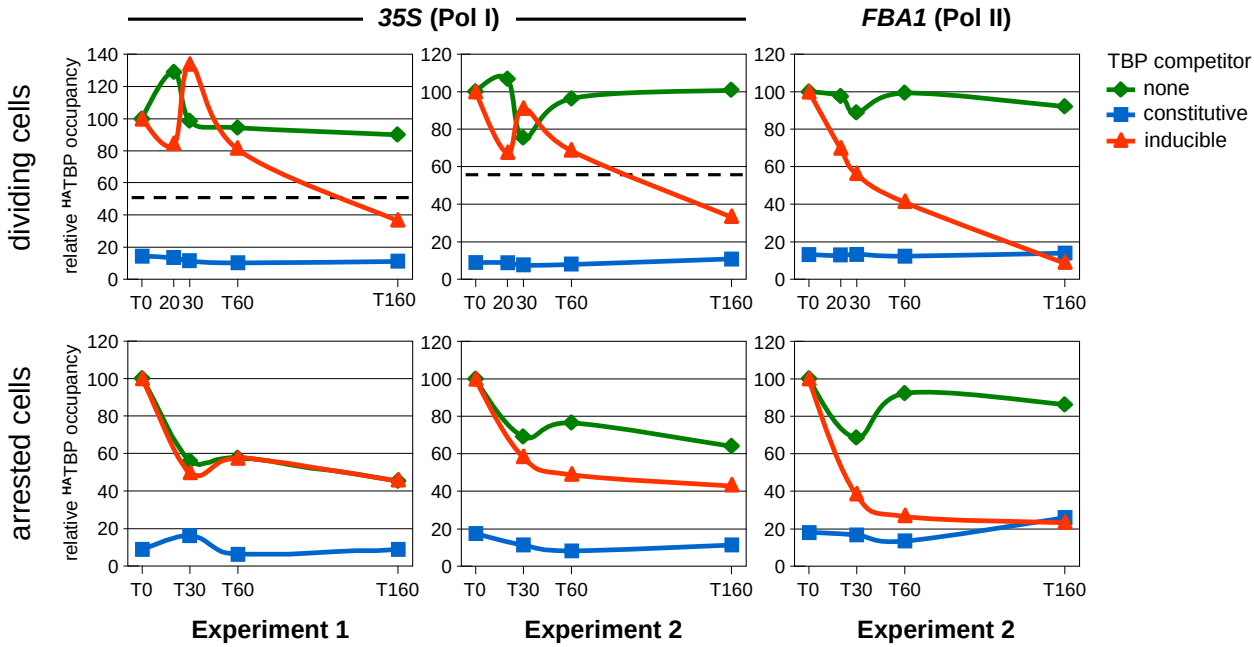
35S (Pol I)
FBA1 (Pol II)
dividing cells
arrested cells
relative HATBP occupancy
140
120
100
80
60
40
20
0
T0 20 30 T60 T160
T0 30 T60 T160
TBP competitor
none
constitutive
inducible
Experiment 1
Experiment 2
Experiment 2

Figure S2. TBP turnover at the *35S* RNA Pol I promoter in dividing cells.

Same competition ChIP experiment as in Figure 1 in exponentially growing cells and, as a control, in G1-arrested cells. Shown are the results of two independent experiments (*Exp 1* and *Exp 2*).

(A) Western blot analysis of galactose-induced expression of the TBP competitor (^{comp}TBP). Galactose was added at T0. Results are presented as in Figure 1C.

(B) Growth rates of the three yeast strains expressing no TBP competitor (*none*), or expressing TBP from the constitutive *DED1* promoter (*constitutive*) or the galactose-inducible *GAL1* promoter (*inducible*). The three strains were grown in parallel. Growth was determined by cell density measurements (OD600). Note that at T160 after galactose addition cells have undergone one cell division.

(C) ^{HA}TBP occupancy at the *35S* RNA Pol I promoter and, as a control, at the *FBA1* RNA Pol II promoter was measured by quantitative ChIP in dividing (upper panels) and G1-arrested (lower panels) cells as in Figure 1. The ChIP signals are relative to those measured at T0 in each strain. These were set to a value of 100, except for the constitutively expressing TBP strain (blue line) for which the T0 value is relative to the signal detected in the strain expressing no TBP competitor. ChIP analysis was performed starting with chromatin samples prepared from the same number of cells at each time point. As a result, the ChIP signal is expected to decrease by 2-fold after one cell division due to dilution if ^{HA}TBP were to remain stably bound at the promoter (dotted line = mean value of the ChIP signals measured at T160 in the strains expressing no and constitutive levels of the TBP competitor). Note that the decrease in ^{HA}TBP occupancy at the *35S* promoter in dividing cells is more pronounced than can be accounted for solely by dilution due to cell division. However, at T160, after one cell division, occupancy does not reach the basal levels detected in cells constitutively expressing TBP (blue line), as is the case for *FBA1*. This suggests that TBP may remain bound at some *35S* promoters during a complete cell cycle.

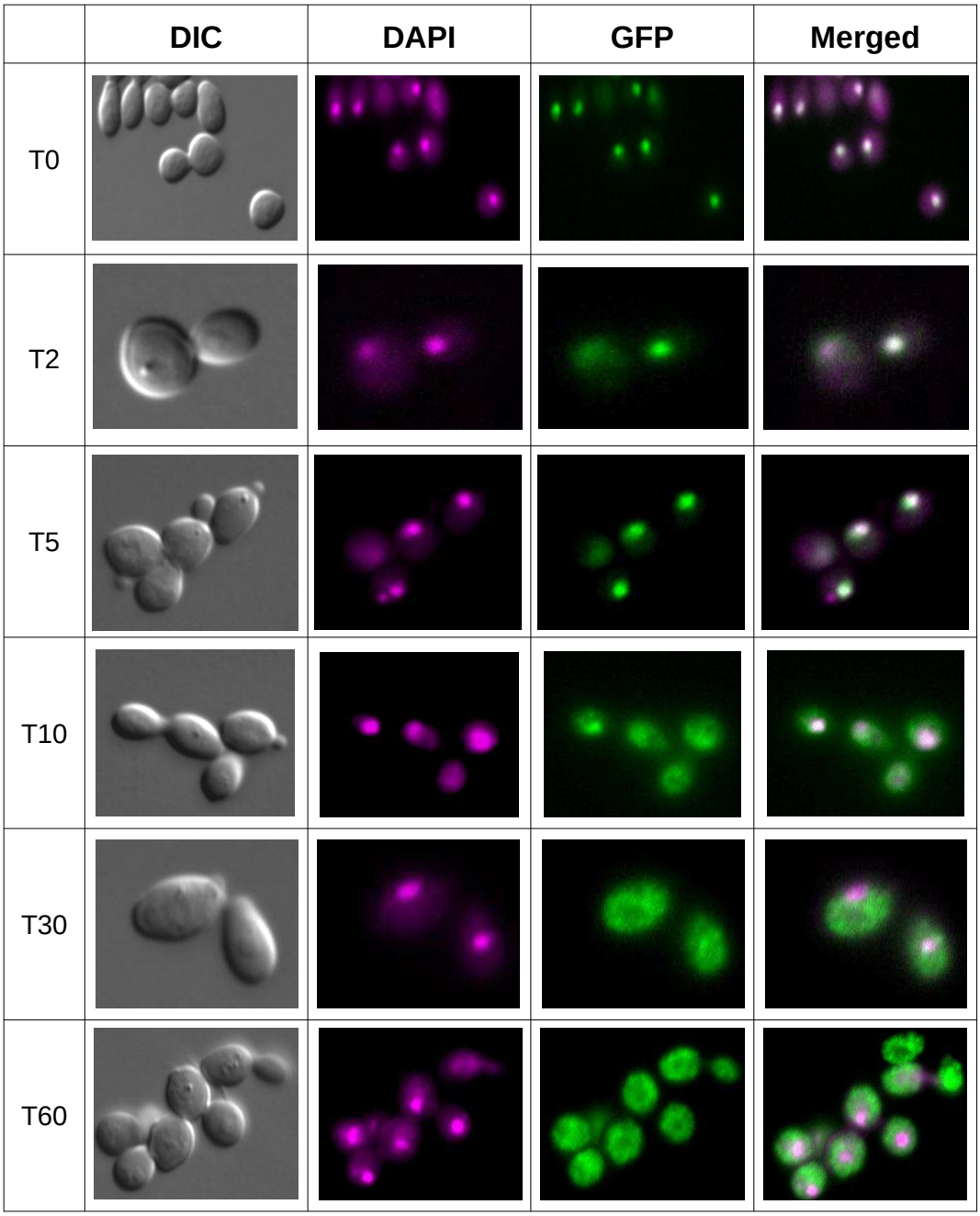

Figure S3. Fluorescence microscopy analysis of TBP-FRB nuclear export.

An exponential culture of an anchor-away strain expressing a GFP-tagged version of TBP-FRB (Haruki et al. 2008. Mol. Cell 31: 925) was treated with rapamycin for the indicated time, fixed and examined for DAPI staining (second column) and GFP fluorescence (third column). Merged images are shown on the right. DIC, differential interference contrast. Note that TBP depletion from the nucleus becomes evident 10 min after addition of rapamycin. This is consistent with the Haruki paper, but clearly slower than the kinetics of TBP disappearance from RNA Pol II promoters as measured by ChIP (see Figure 2). This suggests that rapamycin-mediated binding of TBP to the ribosomal protein anchor suffices to block its association with promoters and/or other basal components prior to its export out of the nucleus

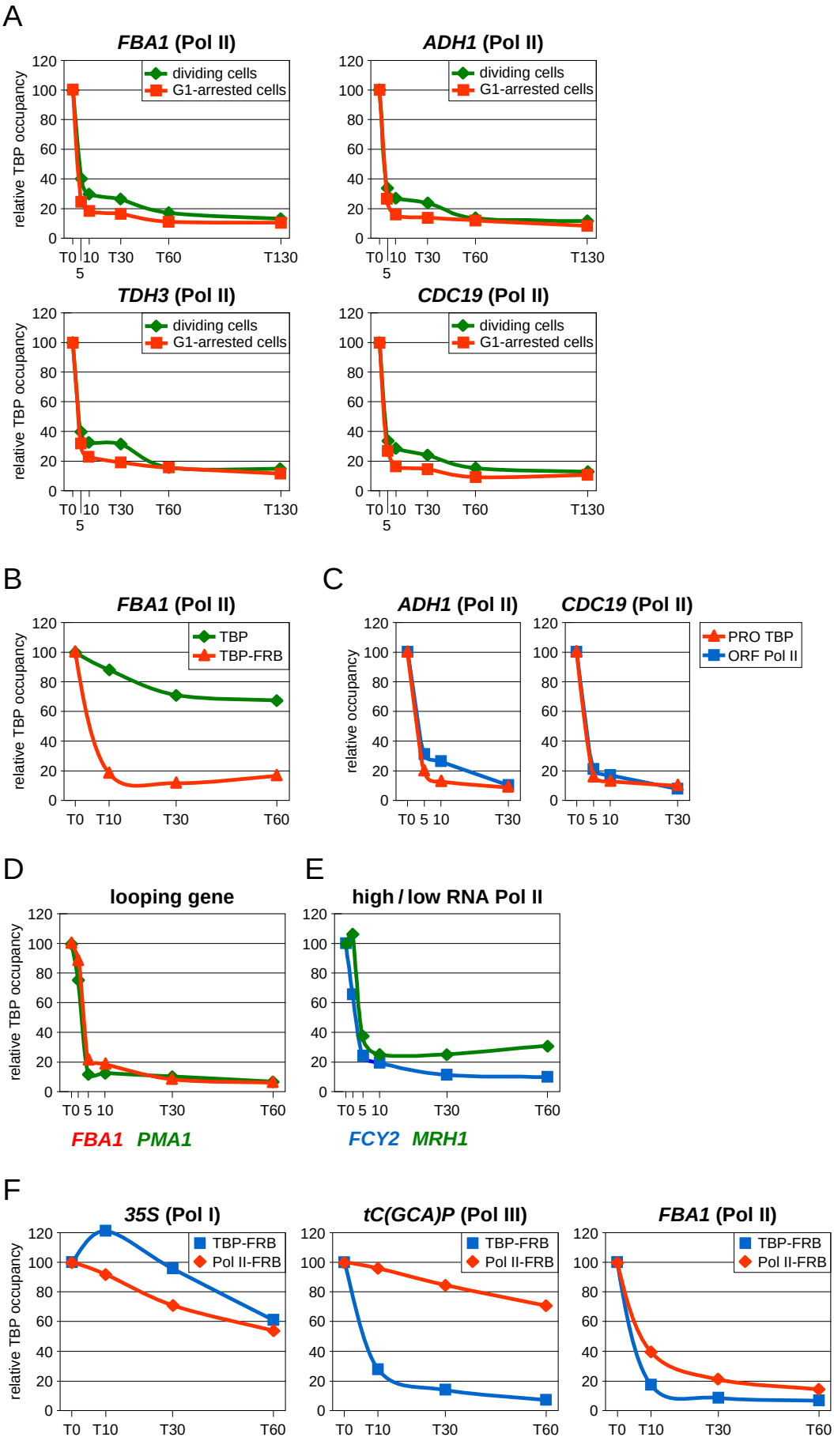
A
FBA1 (Pol II)
ADH1 (Pol II)
TDH3 (Pol II)
CDC19 (Pol II)
dividing cells
G1-arrested cells
relative TBP occupancy
T0
5
10
T30
T60
T130
B
FBA1 (Pol II)
TBP
TBP-FRB
C
ADH1 (Pol II)
CDC19 (Pol II)
PRO TBP
ORF Pol II
relative occupancy
D
looping gene
FBA1
PMA1
E
high / low RNA Pol II
FCY2
MRH1
F
35S (Pol I)
tC(GCA)P (Pol III)
FBA1 (Pol II)
TBP-FRB
Pol II-FRB

Figure S4. TBP and RNA Pol II occupancy after nuclear depletion of TBP by the anchor-away method.

(A) TBP anchor away in dividing versus G1-arrested cells. FRB-tagged TBP occupancy at the indicated promoters and time points after rapamycin addition was determined in exponentially growing and G1-arrested cells by quantitative ChIP as described in Figure 2.

(B) Rapamycin-mediated loss of promoter-bound TBP requires the rapamycin-binding domain FRB. TBP occupancy at the *FBA1* promoter was measured just before (T0) and after addition of rapamycin in two isogenic strains expressing either native TBP (green) or FRB-tagged TBP (red) by quantitative ChIP as in Figure 2.

(C) Loss of TBP at the promoter results in a concomitant loss of RNA Pol II over transcribed regions. ChIP analysis for TBP promoter occupancy (PRO, red line) and RNA Pol II density within the downstream coding region (*ORF*, blue line) after addition of rapamycin at T0 was performed using antibodies against TBP and the large subunit (Rpb1) of the polymerase.

(D) Same experiment as in Figure 2 at the *PMA1* gene reported to form a loop between the promoter and termination regions. The results for *FBA1* are from Figure 2B and serve as a comparison.

(E) Same at two genes with high (*FCY2*) or low (*MRH1*) RNA Pol II promoter occupancy according to Yeast Genome Browser data. See text for details. Note that *MRH1* shows low starting TBP occupancy, which explains the higher values at later time points when expressed relative to the reference T0 value.

(F) TBP occupancy at the indicated RNA Pol I, Pol II and Pol III genes after rapamycin-mediated nuclear depletion of TBP (*TBP-FRB*, blue curves) or RNA Pol II (*Pol II-FRB*, red curves). Note that the same progressive decrease in TBP occupancy is observed at the 35S RNA Pol I promoter under both situations, indicating that this occurs as an indirect consequence of RNA Pol II transcriptional shutdown.

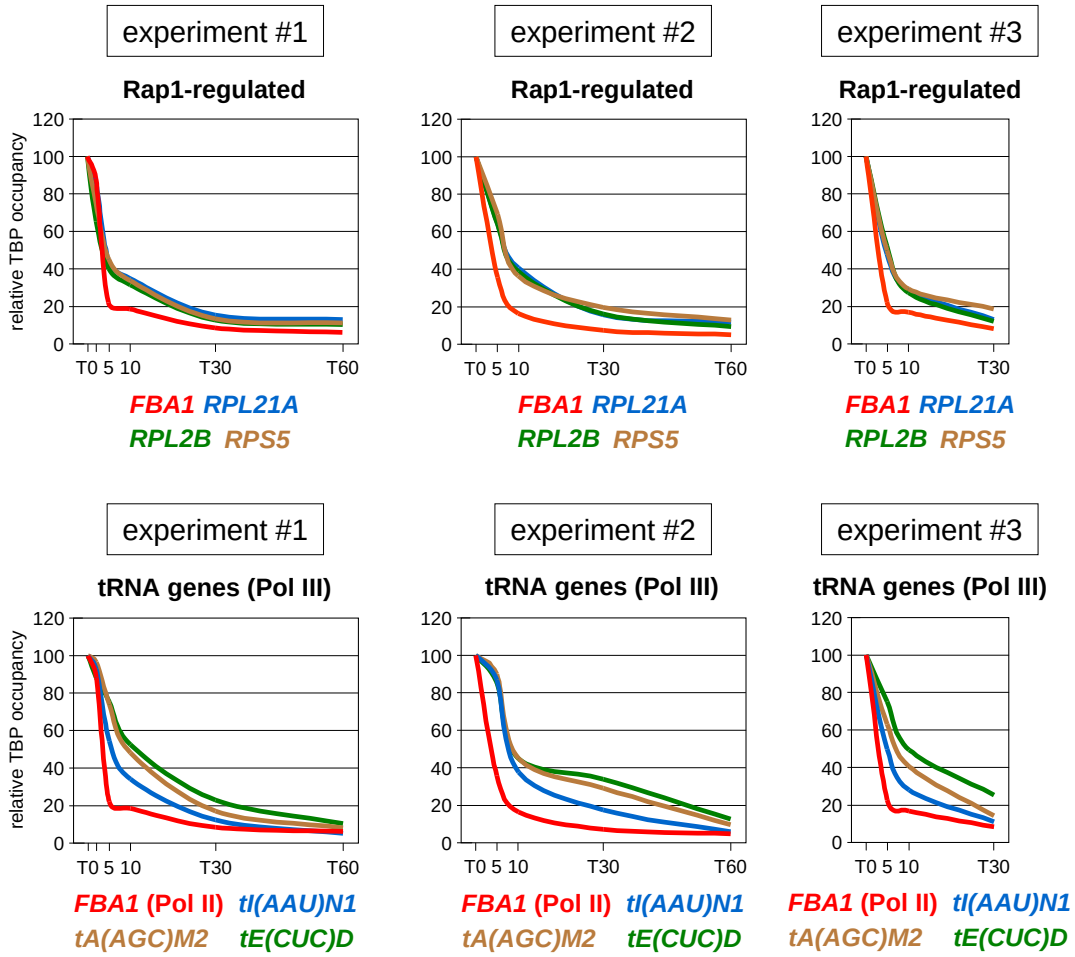

Figure S5. TBP residence time at Rap1-regulated RNA Pol II promoters and at RNA Pol III promoters as measured by the anchor-away assay.

Three independent experiments were performed exactly as described in the legend of Figure 2. The results presented in the upper left panel are the same as in Figure 2E. The results for *FBA1* and the RNA Pol III gene *tE(CUC)D* in Experiment #1 (lower left panel) are from Figure 2B and serve as a comparison. Experiment #1 includes a 2-minute time point. Note that the Rap1-regulated genes and the RNA Pol III genes tested show a slower rate of TBP depletion compared to *FBA1* in all three experiments.

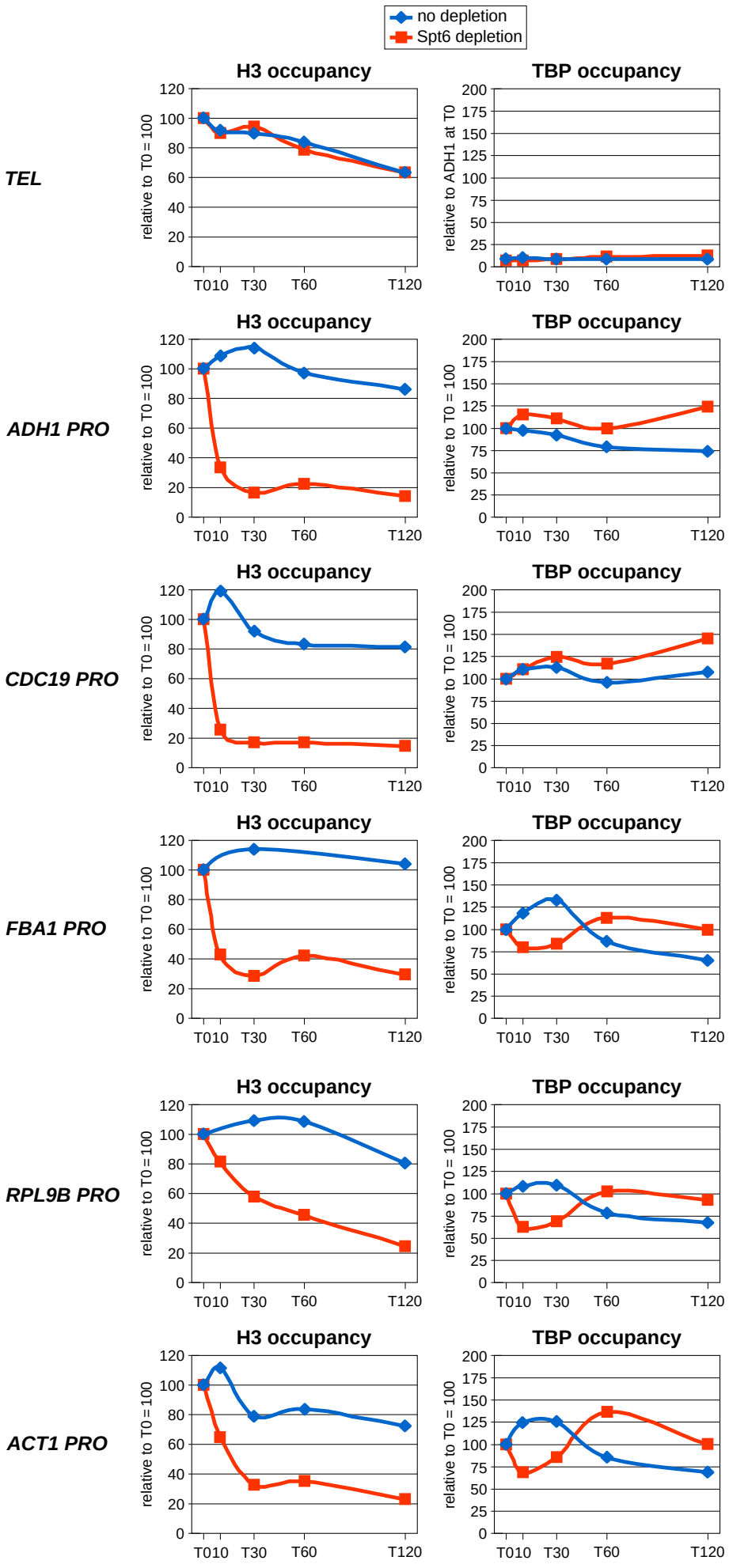
no depletion
Spt6 depletion
TEL
ADH1 PRO
CDC19 PRO
FBA1 PRO
RPL9B PRO
ACT1 PRO
H3 occupancy
TBP occupancy
relative to T0 = 100
relative to ADH1 at T0
T0
10
T30
T60
T120

Figure S6. Nucleosome depletion does not impact on native TBP steady-state occupancy.

Histone H3 (left panels) and TBP (right panels) promoter occupancies were measured at the indicated promoters in the parental anchor-away strain (blue lines) or a derivative expressing FRB-tagged Spt6 (red lines) just before (T0) and at the indicated time points after addition of rapamycin to deplete Spt6 from the nucleus. *TEL* is a subtelomeric region on chromosome VI. ChIP analysis was performed using anti-histone H3 and anti-TBP antibodies as in Figure 3. The values for TBP were divided by those obtained at the same time point at the 35S promoter to correct for variation between samples. The results are expressed relative to the T0 values, which were set to 100, except for TBP at TEL where the T0 value is relative to the signal detected at *ADH1* at the same time point. Note that the TBP ChIP signal at these RNA Pol II promoters is significantly lower (by 5- to 10-fold) than at RNA Pol III promoters, indicating partial occupancy (data not shown; Van Werven et al, 2009). One therefore would expect to see an increase in TBP steady-state occupancy if the average binding duration of TBP were to increase following nucleosome depletion.

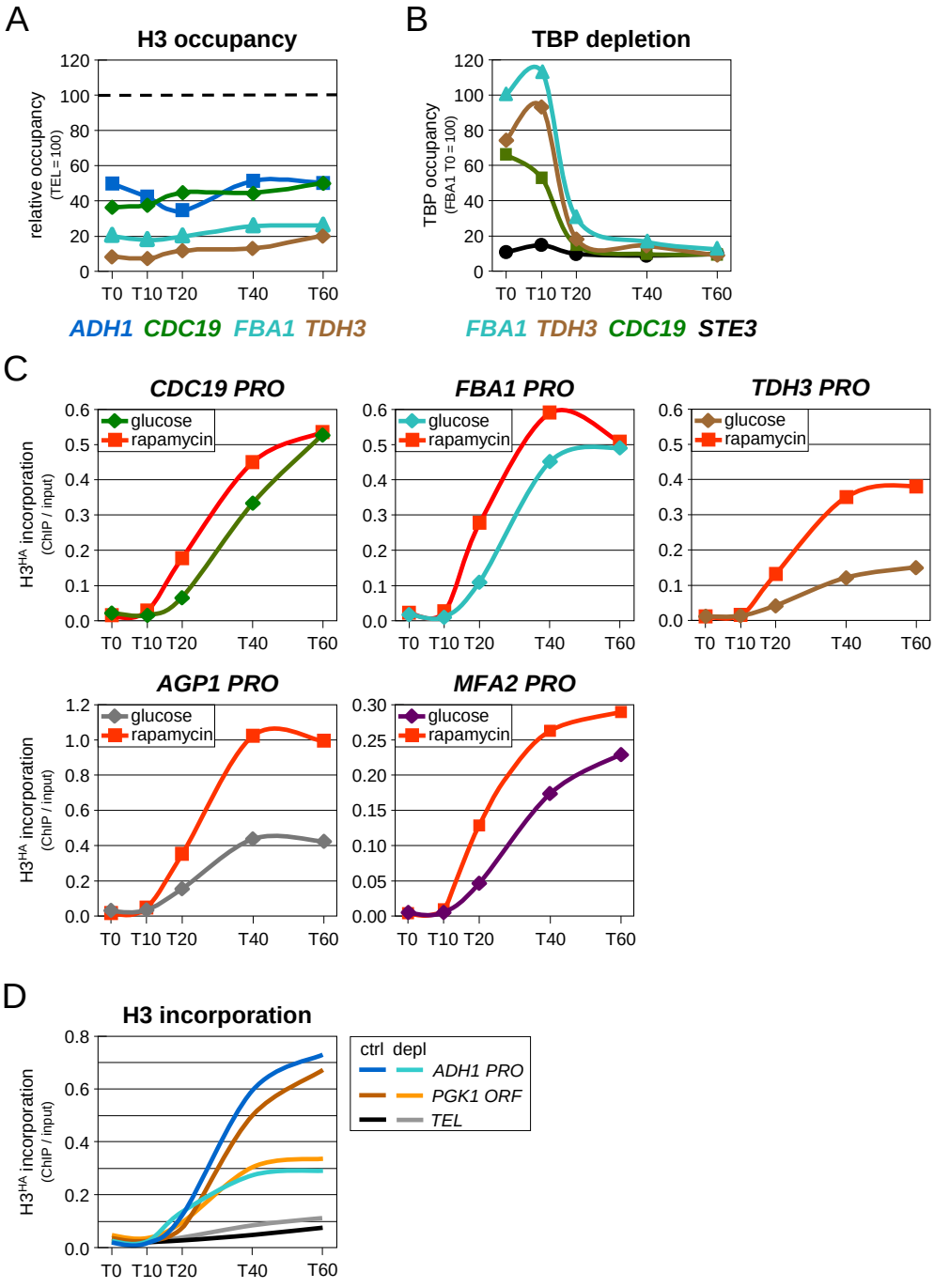
A
H3 occupancy
relative occupancy (TEL = 100)
ADH1 CDC19 FBA1 TDH3
B
TBP depletion
TBP occupancy (FBA1 T0 = 100)
FBA1 TDH3 CDC19 STE3
C
CDC19 PRO
FBA1 PRO
TDH3 PRO
AGP1 PRO
MFA2 PRO
glucose
rapamycin
H3HA incorporation (ChIP / input)
T0 T10 T20 T40 T60
D
H3 incorporation
ctrl depl
ADH1 PRO
PGK1 ORF
TEL

Figure S7. Nucleosome occupancy and turnover upon TBP depletion.

(A) Lack of effect of TBP depletion on promoter nucleosome occupancy. The amounts of histone H3 detected at the indicated promoters in the TBP-anchor-away strain prior to (T0) and after addition of rapamycin to deplete TBP from the nucleus were measured using anti-histone H3 antibodies. The results are expressed relative to the ChIP signals detected at a subtelomeric region on chromosome VI (Jamai et al., 2007) at each time point, which was set to 100 (dotted line).

(B) TBP promoter occupancy prior to and after rapamycin-mediated nuclear depletion at the indicated additional promoters was measured exactly as in Figure 4B. The results for *CDC19* and *STE3* are from Figure 4C. The values are expressed relative to the ChIP signal for *FBA1* at T0, which was set to a value of 100.

(C) $H3^{HA}$ incorporation prior to and after rapamycin-mediated TBP depletion was measured at the indicated additional genes as in Figure 4. The results for the *CDC19* gene promoter are from Figure 4C and are shown for comparison. Note the different scales for *AGP1* and *MFA2*. Also note the higher levels of $H3^{HA}$ incorporation at *ADH1* (Figure 4C) compared to *CDC19* and *FBA1* under control (glucose) conditions and at *AGP1* (red lines) following TBP depletion (red lines). This suggests that the lack of change in $H3^{HA}$ incorporation at *CDC19* and *FBA1* following TBP depletion is not due to limitation in galactose induced $H3^{HA}$ expression.

(D) $H3^{HA}$ incorporation at the *PGK1* transcribed region following depletion of TBP. $H3^{HA}$ incorporation within the *PGK1* open reading frame (*ORF*) under control conditions (dark colors) or after TBP depletion by rapamycin (light colors) was determined as in Figure 4C. The results for the *ADH1* promoter are from Figure 4C. TEL is a subtelomeric region on chromosome VI showing no histone exchange (Jamai et al., 2007). Note that the decrease in $H3^{HA}$ incorporation upon TBP depletion at the *ADH1* promoter is very similar to that observed in the *PGK1* transcribed region. Nucleosome exchange over transcribed regions is only observed at highly expressed genes and is expected to cease when transcription is shut off (Jamai et al., 2007). The remaining $H3^{HA}$ incorporation at the *PGK1* ORF in this experiment may thus be due to some transcription still occurring during the early time points, and the same may be true for TBP binding at the *ADH1* promoter. Nucleosome exchange at the *ADH1* promoter may therefore occur exclusively as a consequence of continuous PIC assembly and disassembly.

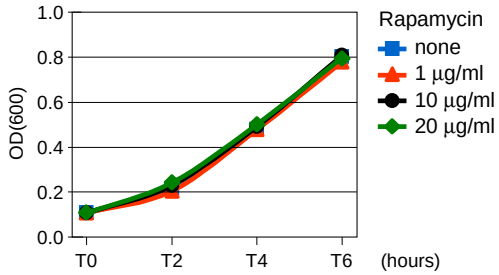

Figure S8. Growth curves of the parental anchor-away yeast strain HHY221 in the presence of the indicated concentrations of rapamycin.